RESEARCH ARTICLE

LpxC Inhibitors as New Antibacterial Agents and Tools for Studying Regulation of Lipid A Biosynthesis in Gram-Negative Pathogens

Andrew P. Tomaras,[a] Craig J. McPherson,[a] Michael Kuhn,[a]* Arlene Carifa,[a] Lisa Mullins,[a]* David George,[a] Charlene Desbonnet,[a] Tess M. Eidem,[b] Justin I. Montgomery,[c] Matthew F. Brown,[c] Usa Reilly,[c] Alita A. Miller,[a]* John P. O'Donnell[a]*

Discovery Biology, Antibacterials Research Unit, Pfizer Worldwide Research and Development, Groton, Connecticut, USA[a]; Department of Microbiology and Immunology, University of Rochester Medical Center, Rochester, New York, USA[b]; Worldwide Medicinal Chemistry, Pfizer Worldwide Research and Development, Groton, Connecticut, USA[c]

* Present address: Alita A. Miller and John P. O'Donnell, Infection Innovative Medicine Unit, AstraZeneca R&D Boston, Waltham, Massachusetts, USA; Michael Kuhn and Lisa Mullins, Zoetis, Kalamazoo, Michigan, USA.

ABSTRACT **The problem of multidrug resistance in serious Gram-negative bacterial pathogens has escalated so severely that new cellular targets and pathways need to be exploited to avoid many of the preexisting antibiotic resistance mechanisms that are rapidly disseminating to new strains. The discovery of small-molecule inhibitors of LpxC, the enzyme responsible for the first committed step in the biosynthesis of lipid A, represents a clinically unprecedented strategy to specifically act against Gram-negative organisms such as *Pseudomonas aeruginosa* and members of the *Enterobacteriaceae*. In this report, we describe the microbiological characterization of LpxC-4, a recently disclosed inhibitor of this bacterial target, and demonstrate that its spectrum of activity extends to several of the pathogenic species that are most threatening to human health today. We also show that spontaneous generation of LpxC-4 resistance occurs at frequencies comparable to those seen with marketed antibiotics, and we provide an in-depth analysis of the mechanisms of resistance utilized by target pathogens. Interestingly, these isolates also served as tools to further our understanding of the regulation of lipid A biosynthesis and enabled the discovery that this process occurs very distinctly between *P. aeruginosa* and members of the *Enterobacteriaceae*. Finally, we demonstrate that LpxC-4 is efficacious *in vivo* against multiple strains in different models of bacterial infection and that the major first-step resistance mechanisms employed by the intended target organisms can still be effectively treated with this new inhibitor.**

IMPORTANCE **New antibiotics are needed for the effective treatment of serious infections caused by Gram-negative pathogens, and the responsibility of identifying new drug candidates rests squarely on the shoulders of the infectious disease community. The limited number of validated cellular targets and approaches, along with the increasing amount of antibiotic resistance that is spreading throughout the clinical environment, has prompted us to explore the utility of inhibitors of novel targets and pathways in these resistant organisms, since preexisting target-based resistance should be negligible. Lipid A biosynthesis is an essential process for the formation of lipopolysaccharide, which is a critical component of the Gram-negative outer membrane. In this report, we describe the *in vitro* and *in vivo* characterization of novel inhibitors of LpxC, an enzyme whose activity is required for proper lipid A biosynthesis, and demonstrate that our lead compound has the requisite attributes to warrant further consideration as a novel antibiotic.**

Received 25 June 2014 **Accepted** 29 August 2014 **Published** 30 September 2014

Citation Tomaras AP, McPherson CJ, Kuhn M, Carifa A, Mullins L, George D, Desbonnet C, Eidem TM, Montgomery JI, Brown MF, Reilly U, Miller AA, O'Donnell JP. 2014. LpxC inhibitors as new antibacterial agents and tools for studying regulation of lipid A biosynthesis in Gram-negative pathogens. mBio 5(5):e01551-14. doi:10.1128/mBio.01551-14.

Editor Liise-anne Pirofski, Albert Einstein College of Medicine

Address correspondence to Andrew P. Tomaras, andrew.tomaras@pfizer.com.

The war against antibiotic resistance rages on for the anti-infective community, as the emergence and spread of mechanisms that effectively subvert the activity of marketed antibacterial agents continue at a terrifying rate. While efforts to fight this battle have been limited in number, there have been valiant attempts to develop new analogs of existing antibiotic classes, with several of these upgraded molecules advancing to clinical trials recently (1–3). And while each of these agents will undoubtedly prove efficacious against many target species, the potential gaps in strain coverage due to the expression of preexisting resistance mechanisms will likely limit their widespread utility, leaving many patients with very few, if any, viable treatment options. As we continue in our quest to identify emerging pathogens and develop new anti-infective agents to combat multidrug-resistant (MDR) strains, antibacterial discovery efforts must be broadened to include the exploration of new cellular pathways, especially since target-based resistance should not exist against clinically unprecedented cellular targets. Although there are multiple examples of this approach, one of the most intriguing and promising novel pathways for the treatment of Gram-negative bacteria is lipid A biosynthesis.

The outer membrane of Gram-negative pathogens, one of the most important features distinguishing them from Gram-positive organisms, has presented a significant challenge to antibacterial drug discoverers due to its remarkable ability to restrict access of

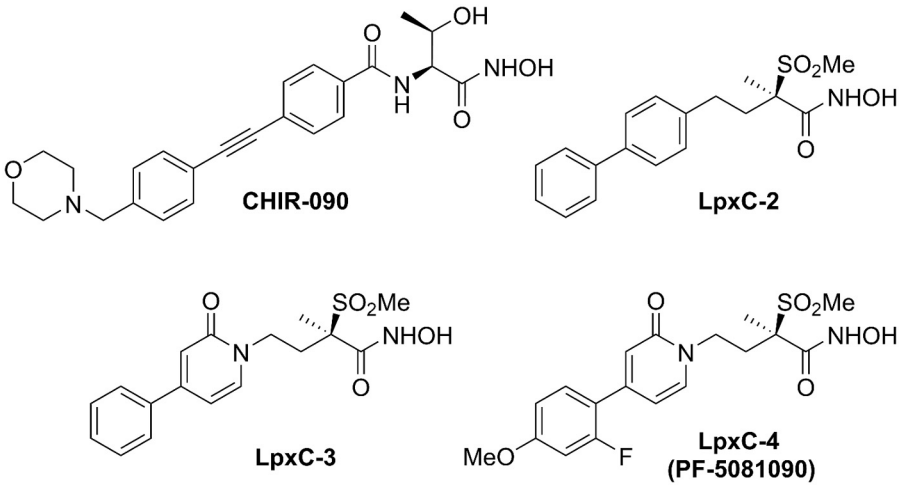

FIG 1 Structures of LpxC inhibitors used in these studies.

small molecules to the periplasmic space (4, 5). In response, novel and innovative approaches to circumvent this impermeability are currently being explored and developed (6, 7); however, their ultimate potential clinical utility remains unknown. As an alternative strategy, many groups have elected to exploit outer membrane biogenesis pathways to find new antibiotic targets. Among the various components that are responsible for outer membrane assembly, the synthesis of lipid A molecules is among the most critical, since these moieties serve as the anchor on the outer membrane for lipopolysaccharide (LPS) attachment. For most Gram-negative organisms, the inability to decorate the outer membrane with LPS has a bactericidal effect, and thus the interference of lipid A biosynthesis by a small-molecule inhibitor would prevent LPS assembly and result in the death of the target bacterial cell. The UDP-3-*O*-(*R*-3-hydroxymyristoyl)-*N*-acetylglucosamine deacetylase, encoded by *lpxC*, represents the first committed step in the lipid A biosynthetic pathway and has emerged as a novel antibiotic target for the treatment of Gram-negative infections (8–10).

Here we report the advancement of novel classes of LpxC inhibitors and provide an in-depth characterization of a lead compound, LpxC-4, in terms of its microbiological spectrum, resistance potential, and *in vivo* efficacy. Through the course of our investigation, using spontaneously resistant isolates generated during these profiling efforts, we identified several unexpected physiological responses that differed among the various Gram-negative pathogens we are targeting. In addition, we show that LpxC-4 still retains efficacy against mutants expressing these different first-step resistance mechanisms, demonstrating the potential clinical utility of this inhibitor class.

RESULTS

LpxC inhibitors are potent and rapidly bactericidal against multiple Gram-negative species. Our efforts to identify a potent, broad-spectrum inhibitor of LpxC have focused on a Zn^{2+} binding class of hydroxamic acids. The structures of the lead molecules from two different series of compounds are shown in Fig. 1. LpxC-2, one of our leads from the biphenyl methylsulfone-containing series, has been described previously (11), as have the pyridone-substituted compounds LpxC-3 and LpxC-4 (12). While the 50% inhibitory concentrations (IC_{50}s) for each of these compounds against the *Pseudomonas aeruginosa* LpxC enzyme are not substantially different, the pyridone analog LpxC-4 demonstrates a clear MIC_{90} advantage over the biphenyl analog LpxC-2 when tested against a panel of 106 recent clinical isolates (Table 1). By comparison, despite it having enzyme inhibitory activity roughly equivalent to that of LpxC-4, the MIC_{90} of CHIR-090, a highly potent LpxC inhibitor that is active against a wide variety of MDR Gram-negative bacteria (13, 14), was found to be 4-fold higher against *P. aeruginosa*. In the case of *Klebsiella pneumoniae*, an ~10-fold decrease in the enzyme IC_{50} between LpxC-3 and LpxC-4 resulted in a 16-fold decrease in MIC_{90} to 1 μg/ml (Table 1). In *Acinetobacter baumannii*, however, all LpxC inhibitors tested had considerably higher enzyme IC_{50}s and MIC_{90} values that were 32 μg/ml or greater. It should be noted, however, that a structurally related LpxC inhibitor from the pyridone class was recently demonstrated to have significant *in vivo* efficacy against an MDR clinical isolate of *A. baumannii* despite having no whole-cell activity *in vitro* (15), a disconnect which is likely due to the unusual ability of *A. baumannii* to survive *in vitro* without LPS (16). Many of our compounds, most notably LpxC-4, also have strong activity against other important Gram-negative species, including *Escherichia coli*, *Enterobacter* spp., *Burkholderia cepacia*, and *Stenotrophomonas maltophilia* (Table 1). Since it proved to be a potent compound with broad-spectrum activity, we chose to further characterize LpxC-4 both *in vitro* and *in vivo*.

We first conducted standard static time-kill (STK) studies using LpxC-4 concentrations which targeted multiples above and below the MIC against representative strains of *P. aeruginosa* and *K. pneumoniae*. Figure 2A shows the rapid bactericidal activity of LpxC-4 against *P. aeruginosa* UC12120, with regrowth limited to drug concentrations of ≤2× the MIC (0.25 μg/ml). The kill rate is not as dramatic against the cystic fibrosis (CF) clinical isolate PA-1955, which constitutively expresses the *mexEF-oprN* efflux pump (Fig. 2B). While regrowth is still restricted to drug concentrations of ≤2× the MIC (4 μg/ml) and stasis is seen at 4× the MIC, the kinetics of bacterial killing is considerably slower than that observed with UC12120, which suggests that efflux upregulation may play a role in this phenotype, as has been described previously (11). Testing of a recent, KPC-producing clinical isolate of

TABLE 1 In vitro microbiological assessment of novel LpxC inhibitors shows superior activities against a broad spectrum of Gram-negative pathogens compared to CHIR-090 and meropenem

Bacterium (n[a])	Activity of:								
	LpxC-2[b]		LpxC-3[c]		LpxC-4		CHIR-090		MPM[d]
	IC_{50} (nM)	MIC_{90} (μg/ml)	IC_{50} (nM)	MIC_{90} (μg/ml)	IC_{50} (nM)	MIC_{90} (μg/ml)	IC_{50} (nM)	MIC_{90} (μg/ml)	MIC_{90} (μg/ml)
P. aeruginosa (138)	1.4	4	3.6	2	1.1	1	<2.1	4	>64
P. aeruginosa PAO1 WT[e]	1.4	0.5	3.6	0.5	1.1	0.5	<2.1	1	0.25
P. aeruginosa PAO1 M62R	7.9	4	2.8	0.5	2.1	0.5	NT	NT	NT
K. pneumoniae (98)	1.0	16	0.68	16	0.069	1	NT	NT	32
E. coli (79)	NT[f]	2	NT	8	NT	0.25	NT	0.25	NT
Enterobacter spp. (52)[g]	NT	4	NT	16	NT	0.5	NT	0.5	0.25
A. baumannii (31)	>41	32	110	32	183	>64	NT	>64	32
B. cepacia (30)	NT	NT	NT	NT	NT	0.5	NT	>64	8
S. maltophilia (30)	NT	NT	NT	NT	NT	2	NT	>64	>64

[a] n, no. of isolates.
[b] MIC data from reference 11.
[c] MIC data from reference 12.
[d] MPM, meropenem.
[e] WT, wild type.
[f] NT, not tested.
[g] Includes 21 *E. aerogenes* and 31 *E. cloacae* isolates.

K. pneumoniae, however, demonstrated the same pattern of rapid bactericidal activity as was seen with UC12120, with no regrowth seen at concentrations of 4× the MIC or higher (Fig. 2C).

LpxC-4 resistance in *P. aeruginosa*, although infrequent, arises from efflux pump and/or target upregulation. In order to assess the resistance emergence potential for our lead LpxC inhibitors, we used standard frequency-of-resistance (FOR) methods with representative strains of *P. aeruginosa* and *K. pneumoniae*. *P. aeruginosa* resistance frequencies, which were calculated based on LpxC-4 concentrations above each strain's respective MIC and are shown in Table 2, demonstrate that each of the strains tested has an extremely low probability of developing spontaneous resistance to LpxC-4. In addition, several resistant isolates were recovered, and their MICs relative to that for the parent strain were determined. For *P. aeruginosa* PAO1 and UC12120, a 2- to 4-fold increase in the LpxC-4 MIC relative to that of each respective parent strain was observed (Table 2). Spontaneously resistant *P. aeruginosa* PA-1955 isolates, however, showed a much more pronounced MIC shift relative to findings for the parent strain (8- to 32-fold). Cross-resistance MIC profiling of the *P. aeruginosa* LpxC-4^R isolates demonstrated that quinolone resistance was increased as well (data not shown), which prompted our evaluation of LpxC-4 MICs against these resistant isolates in both the presence and absence of the efflux pump inhibitor PAβN. Addition of 50 μg/ml PAβN fully restored the LpxC-4 MIC to parental levels in all PAO1 and UC12120 resistant isolates tested while only partially reducing the MICs of PA-1955 isolates (Table 2).

Our preliminary MIC results led us to probe total cell extracts of both wild-type and LpxC-4^R mutant strains using Western blot analysis with OprM-, OprN-, and OprJ-specific monoclonal antibodies. Interestingly, while PAO1 mutants showed increased production of OprM relative to results for the parental strain, all resistant UC12120 isolates produced OprN, whereas the parent strain did not (Table 2). Additionally, we noted that the PAO1 resistance frequency was approximately 10-fold lower than that of UC12120. One likely explanation for the differential frequency and mechanistic response seen between these two strains is the existence of a P195T point mutation in the PAO1 *mexT* gene, which encodes the positive regulator of the *mexEF-oprN* operon. While this particular mutation has not been described previously, an 8-bp insertion within this coding region which results in a frame shift that prevents the activation of this efflux system has been described (17). We have speculated that this point mutation similarly prevents the activation of *mexEF-oprN*, as evidenced by the lack of FOR-generated PAO1 mutants that express this efflux pump. In the context of LpxC-4 resistance, this would therefore create a requirement for an alternative efflux system to be activated or upregulated. No changes in efflux expression were detected in the LpxC-4^R PA-1955 isolates relative to that of the parent strain, which constitutively expresses *mexEF-oprN* by virtue of a G78S point mutation encoded in *mexS*, which has previously been described to be involved with activation of this efflux pump (18). OprJ expression was not detected in any *P. aeruginosa* isolate tested.

Additionally, we noted that no mutants with mutations within the *lpxC* coding region were recovered. Previous resistance frequency experiments performed with LpxC-2 yielded mutants that harbored an M62R active site point mutation, resulting in an 8-fold increase in the LpxC-2 MIC (Table 1). The MIC shift associated with this particular mutation was explained by the ~5-fold increase in the IC_{50} for the M62R mutant enzyme versus that for the wild-type version, and backcrossing of this mutation into a wild-type, susceptible *P. aeruginosa* strain recapitulated the level of LpxC-2 resistance seen in the spontaneously generated mutant (data not shown). Encouragingly, the LpxC-4 IC_{50} of the M62R mutant enzyme was not significantly elevated, and correspondingly, no MIC increase against LpxC-4 was seen with this mutant strain (Table 1), which would explain our inability to recover such a mutant in FOR studies. The mutation replaces a relatively nonpolar residue (methionine) with a polar residue (arginine), and based on the known binding mode of the pyridone-containing inhibitors for wild-type LpxC (12), the amino acid side chain of both wild-type and M62R mutant enzymes is likely located near the pyridone carbonyl of LpxC-3 and LpxC-4. This may enable a

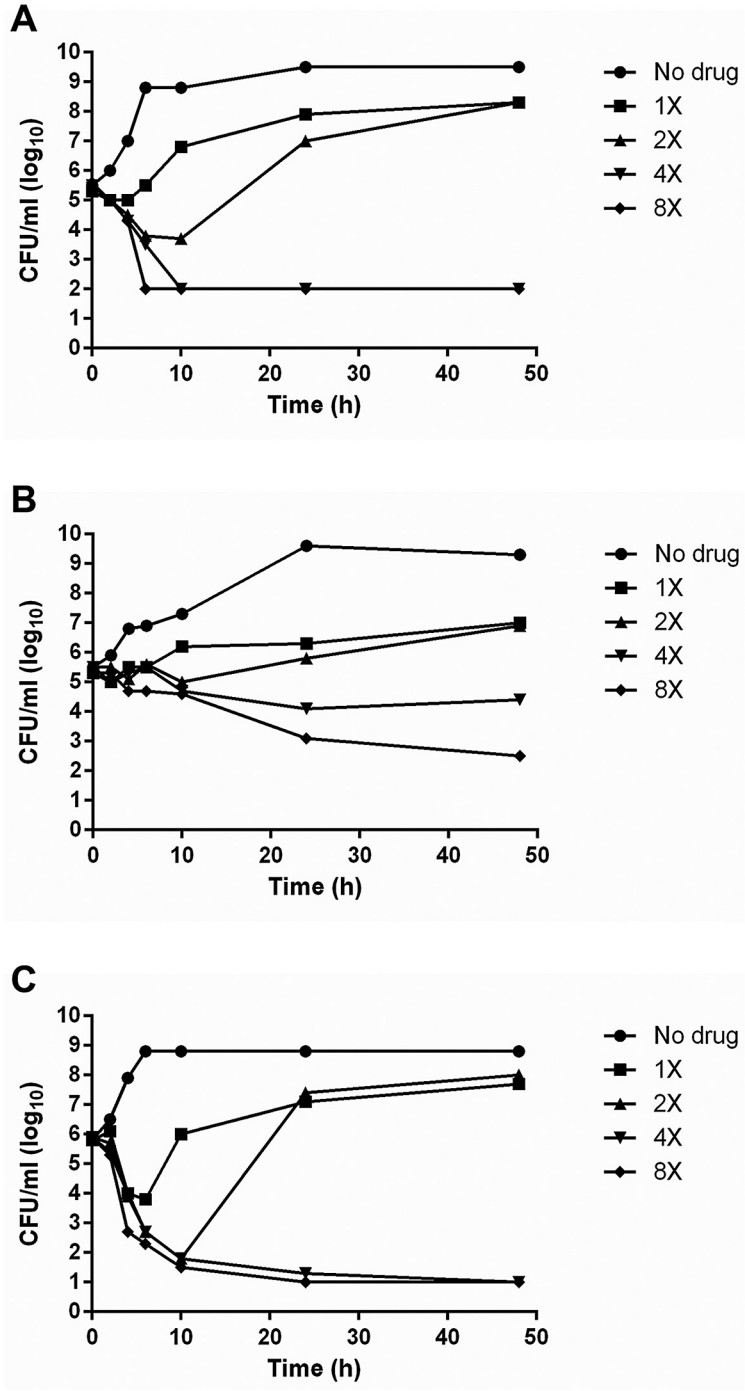

FIG 2 Static-time-kill assays demonstrate sustained bactericidal activities of LpxC-4 against *P. aeruginosa* UC12120 (A), PA-1955 (B), and *K. pneumoniae* KP-1487 (C).

productive H-bonding interaction of these inhibitors with the mutant arginine, thereby maintaining enzyme inhibitory activity. Since LpxC-2 contains a nonpolar phenyl group at this position, a similar productive interaction is not feasible, which may explain the minor loss of activity against the mutant enzyme. Taken together, these FOR results suggest that activation of *mexEF-oprN* is the preferred first-step mechanism employed by *P. aeruginosa* to resist the activity of LpxC-4, although utilization of MexAB-OprM can compensate if the former cannot be activated, albeit at a lower frequency.

To further confirm these preliminary mechanistic findings, we conducted whole-genome sequencing of four PAO1 LpxC-4^R isolates. Given the Western blot results described above, it was not surprising to find that all of these mutants had mutations in *mexR* (Table 2), the repressor of the *mexAB-oprM* operon (19). Sequencing of *mexST* from four resistant UC12120 isolates revealed

TABLE 2 LpxC-4 resistance frequencies are similar in *P. aeruginosa* and *K. pneumoniae*, but resulting first-step mechanisms of resistance are functionally distinct

Strain	FOR (fold MIC)	Resistant isolate no. (genetic alteration)	MIC (μg/ml)		Western blot analysis result			Genotype
			LpxC-4[e]	LpxC-4 + PAβN	OprM	OprN	LpxC	
P. aeruginosa								
PAO1[a] (OprM$^+$)	3.4×10^{-8} (2×)	1	4	0.5	+++	−	+	MexR frameshift at bp 106
	$<5.0 \times 10^{-10}$ (4×)	2	4	0.5	+++	−	+	MexR premature stop codon at Q55
		3	2	0.5	+++	−	+	MexR R82P
		4	2	0.5	+++	−	+	MexR L131Q
UC12120[b] (OprN-)	2.5×10^{-8} (2×)	1	4	1	+	+	+	MexT G258D
	4.2×10^{-9} (4×)	2	4	1	+	+	+	MexS L46F
		3	4	1	+	+	+	MexT G258D
		4	4	1	+	+	+	MexS R322W
PA-1955[c] (OprN+)	1.5×10^{-8} (4×)	1	16	2	+	+	+	ND
	2.5×10^{-10} (8×)	1 (Δ*oprN*)	2	ND[f]	+	−	+	ND
		2	16	1	+	+	+	ND
		2 (Δ*oprN*)	2	ND	+	−	+	ND
		3	16	1	+	+	+	ND
		3 (Δ*oprN*)	2	ND	+	−	+	ND
		4	16	2	+	+	+	ND
		4 (Δ*oprN*)	2	ND	+	−	+	ND
		5	64	8	+	+	+++	C-to-A mutation 11 bp upstream of *lpxC*
		5 (Δ*oprN*)	16	ND	+	−	+++	ND
		6	64	8	+	+	+++	C-to-A mutation 11 bp upstream of *lpxC*
		6 (Δ*oprN*)	16	ND	+	−	+++	ND
K. pneumoniae								Genotype
KP-1487[d]	9.6×10^{-8} (8×)	1	8	4			+	FabZ A78V
	2.2×10^{-9} (16×)	2	16	8			+	FabZ R121L
		3	8	8			+	FabZ P22L
		4	8	4			+	FabZ A78V
		5	8	8			+	FabZ P22S
		6	8	8			+	FabZ P22L

[a] PAO1 MIC = 0.5 μg/ml.
[b] UC12120 MIC = 1 μg/ml.
[c] PA-1955 MIC = 2 μg/ml.
[d] KP-1487 MIC = 1 μg/ml.
[e] For KP-1487, a skipped-well phenomenon was seen at 0.25, 0.5, and 1 μg/ml, MIC reported per CLSI guidelines.
[f] ND, not determined.

that two harbored the exact same point mutation in *mexT*, while the other two each had unique point mutations in *mexS* (Table 2). We then generated *oprN* deletion mutations in multiple resistant UC12120 isolates and found that the LpxC-4 MICs of these isogenic mutants had returned to wild-type UC12120 levels. We also made *oprN* deletion mutants in six PA-1955 LpxC-4^R isolates, but unlike the case with UC12120 mutants, the MICs from only four of the six fully reverted to wild-type levels (Table 2). To help understand the additional mechanism(s) of LpxC-4 resistance potentially being employed in the other two PA-1955 mutants, we sequenced the *lpxC* gene and also performed Western blot analyses using a *P. aeruginosa* LpxC-specific monoclonal antibody. The results of these assays, shown in Table 2, demonstrated that while neither of these isolates had any detectable mutations within the *lpxC* coding region, they both demonstrated increased levels of LpxC production relative to those of both the parental strain and the other four LpxC-resistant mutants. Since increased LpxC production has been described previously as a *P. aeruginosa* resistance

mechanism against other LpxC inhibitors (10), we sequenced the upstream noncoding region of the *lpxC* gene and identified the same C-to-A mutation 11 bp upstream of the translation initiation site in both of these isolates (Table 2).

A *P. aeruginosa*-specific sRNA may contribute to LpxC production and resistance to LpxC inhibitors. The repeated isolation of spontaneous LpxC inhibitor-resistant mutants harboring this upstream, noncoding region mutation, both by our group and by others (10), prompted us to further probe this mechanism of LpxC-4 resistance. We started by backcrossing this mutated allele into PAO397, an engineered PAO1 strain that lacks 5 different RND efflux pumps, so that the contributions of efflux to LpxC-4 resistance would not factor into our analyses. As expected, backcrossing of the C-to-A mutation 11 bp upstream of the *lpxC* translational start resulted in a 16-fold increase in the LpxC-4 MIC relative to that of the parent strain (data not shown). Examination of the DNA sequence upstream of the ribosome binding site (RBS) suggested that a structural element may exist within this region. Computational analysis of this sequence using the mfold server (20) predicted the existence of a small RNA (sRNA) that spans nearly the entire intergenic region separating *lpxC* from *ftsZ*, the gene immediately upstream. Interestingly, this sRNA was recently identified computationally, and its existence was confirmed experimentally by reverse transcription-PCR (RT-PCR) (21, 22), which has led to the naming of this region as PA4406.1 in the PAO1 genome annotation on the *Pseudomonas* Genome Database (23).

Figure 3A shows the predicted structure of the sRNA encoded by wild-type PAO1. In this model, the cytosine 11 bp upstream of the *lpxC* translational start (filled arrow) is part of a hairpin structure that pairs with the guanine 18 bp upstream of *lpxC* (open arrow). Changes to this structure when the C-to-A mutation is introduced are shown in Fig. 3B. Given the relatively simplistic nature of this hairpin, we were skeptical about its contribution to regulation of LpxC translation. Unfortunately, our attempts to further characterize this sRNA by restoring the hairpin structure in the mutant through the introduction of a G-to-T mutation 18 bp upstream of *lpxC* were unsuccessful. Likewise, the cloning of this sRNA into *E. coli* also did not prove successful, at least not without identifying additional mutations elsewhere within the structure. We were able to demonstrate one key difference between the wild-type and C-to-A mutant strains, however. Although this mutation has historically been regarded as one that impacts translation of LpxC both by us and by others (10), we speculated that the position of this mutation within the sRNA coding region could actually be affecting the transcription or mRNA stability of *lpxC*. While quantitative RT-PCR (qRT-PCR) experiments using RNA from wild-type PA-1955, PAO397, and their respective C-to-A mutants did not demonstrate any significant differences in mRNA turnover (data not shown), we were encouraged to see a 3-fold increase in *lpxC* expression in both mutant strains relative to that in their respective parent strains (Fig. 4). While future work is needed to identify any additional components of this regulatory circuit, to our knowledge this is the first report describing a molecular mechanism controlling LpxC production in *P. aeruginosa*.

Curiously, we have yet to identify an LpxC-overproducing mutant from any *P. aeruginosa* isolate that does not already have an efflux pump upregulated, whereas in strains like PA-1955, which constitutively expresses MexEF-OprN, this genotype was found among the few stably resistant spontaneous mutants recovered in FOR experiments. Further supporting this preliminary finding, we were also able to recover mutants with increased levels of LpxC production in a *P. aeruginosa* clinical isolate that overexpresses *mexAB-oprM* (data not shown). As with PA-1955 LpxC-overexpressing mutants, these mutants also contained the C-to-A mutation 11 bp upstream of the *lpxC* translational start. This interesting finding prompted us to perform larger-scale studies by examining 96 FOR-generated mutants from strains expressing efflux pumps at a basal level (such as PAO1 and UC12120). The resulting isolates have demonstrated that efflux upregulation is their primary mechanism of resistance to LpxC inhibitors by virtue of the full restoration of the MIC to wild-type levels when PAβN is included in the assay (data not shown). This suggests that strains that do not have upregulated efflux pumps would require two independent mutational events to become resistant to our LpxC inhibitors to levels that are not predicted to be clinically achievable. To evaluate the resistance propensity from hypermutable *P. aeruginosa* strains, we constructed Δ*mutS* deletion mutants of both PAO1 and UC12120, which resulted in the expected phenotype as assessed by a sharp increase in the rate of spontaneous rifampin resistance. A corresponding increase in the frequency of LpxC-4 resistance was not detected in either of these hypermutable strains, however, and the mechanisms behind the resistance in recovered isolates were no different from those found in wild-type PAO1 and UC12120 (data not shown).

Mutation of *fabZ* is the major first-step LpxC-4 resistance mechanism in the *Enterobacteriaceae*. The LpxC-4 FOR for KP-1487, a KPC-expressing, MDR *K. pneumoniae* clinical isolate, is shown in Table 2. Resistant isolates from this strain, which were recovered at frequencies similar to those with *P. aeruginosa*, showed an 8-fold increase in the MIC relative to that of the parent strain. In contrast to *P. aeruginosa*, however, we noticed a highly reproducible "skipped-well phenomenon" (e.g., bacterial growth at drug concentrations below the parental strain MIC, followed by a gap in growth surrounding concentrations equivalent to the parental strain MIC, followed by growth at higher concentrations) when many of these resistant isolates were profiled by MIC testing. This phenotype has been reported previously (24), although in that particular report it was described in the context of colistin and polymyxin B MIC testing of *Acinetobacter* clinical isolates, as opposed to isogenic resistant mutants whose parent strain does not display this pattern of growth. The skipped-well MIC phenomenon has also been described for *P. aeruginosa* (25), where it was demonstrated that isogenic polymyxin B-resistant mutants can adapt to particular concentrations of this antibacterial agent. To the best of our knowledge, however, this phenomenon has not been described in the context of LpxC inhibitors. While we have reported the MICs of these FOR-generated mutants as 8 μg/ml (Table 2), we also noted that the concentration required to inhibit the growth of wild-type KP-1487 (1 μg/ml) was within the "skipped-well" range when its isogenic mutants were tested, meaning that this concentration was sufficient to kill both wild-type and mutant strains.

The MICs of these resistant isolates were not reduced to parental levels when PAβN was included, nor were these isolates cross-resistant to quinolone antibiotics (data not shown). Both of these phenotypes suggested that efflux pump upregulation/activation was not mediating LpxC-4 resistance in *K. pneumoniae*. Each of these mutants did display cross-resistance to LpxC-2 and LpxC-3,

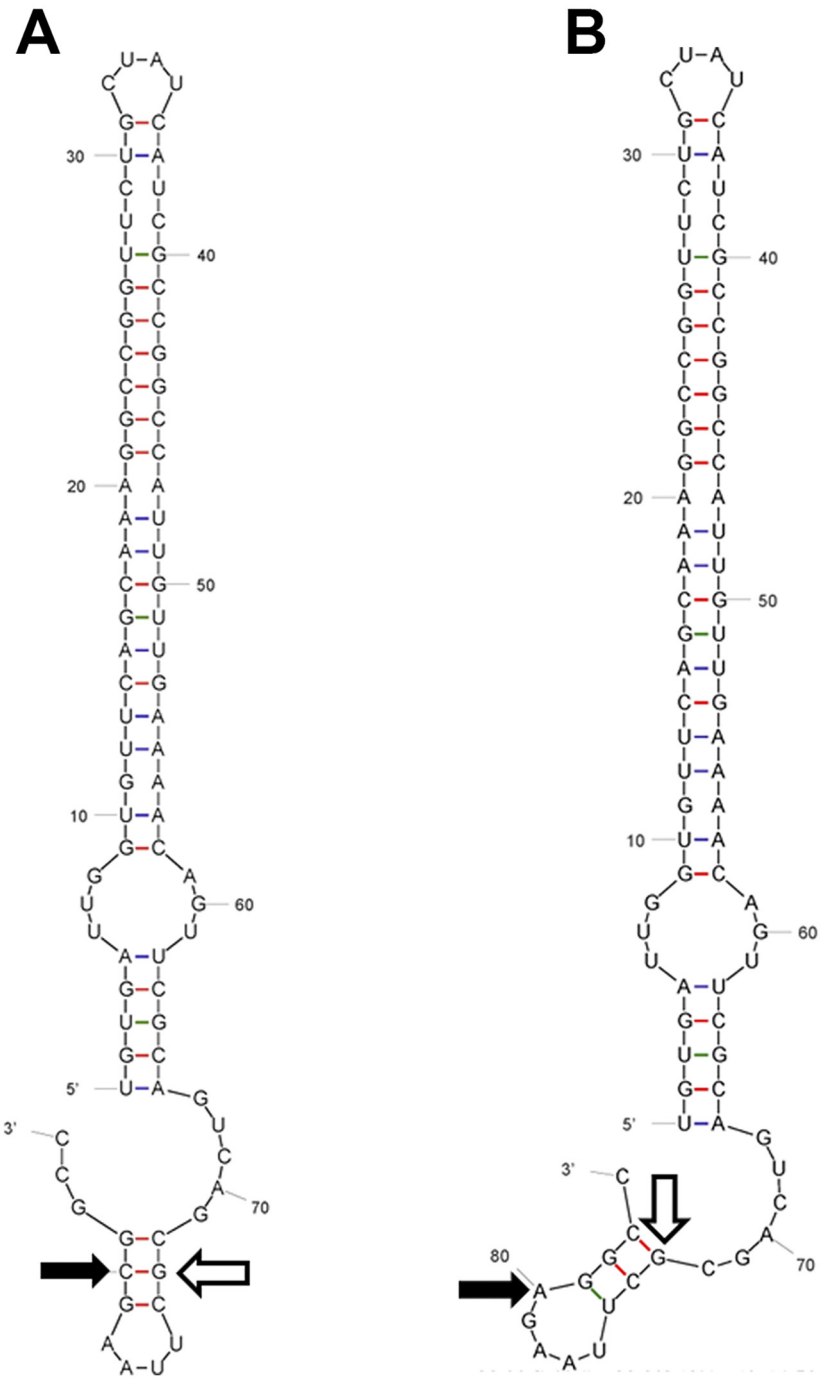

FIG 3 The sRNA predicted to be encoded in the upstream region of *lpxC* in *P. aeruginosa* adopts an altered conformation upon mutation, conferring LpxC-4 resistance. Sequences from the wild-type (A) or C-to-A-mutated (B) variants were analyzed using mfold. The closed arrow indicates the −11 position, while the open arrow indicates the −18 position.

however, which prompted us to explore other potential resistance mechanisms related to the target. First, we sequenced the entire *lpxC* gene from 6 LpxC-4^R KP-1487 isolates, which did not reveal any mutations in this region relative to sequence of the parent strain. The lack of *lpxC* upregulation was confirmed by preparing whole-cell extracts of these strains and performing Western blot analyses using a *K. pneumoniae* LpxC-specific polyclonal antibody (Table 2). Given the previous discovery of *fabZ* mutations correlating with resistance to LpxC inhibitors (10, 26), we next decided to sequence this gene from our resistant mutants. Sequencing of the 6 mutants described above revealed that each harbored a single point mutation in *fabZ* (Table 2), at least one of which has been described previously (26). We subsequently performed whole-genome sequencing and confirmed that these point mutations were the only ones evident in these resistant strains (data not shown).

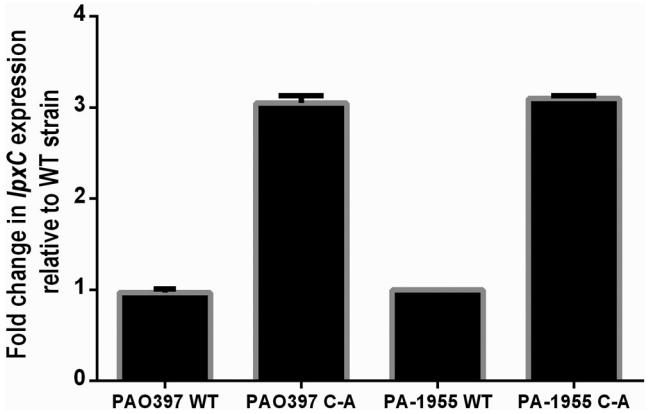

FIG 4 Mutation of the sRNA upstream of *lpxC*, which confers high-level resistance to LpxC-4, results in an increased level of *lpxC* transcription as assessed by qRT-PCR.

***In vivo* efficacy against wild-type *P. aeruginosa* and *K. pneumoniae* strains is translatable from *in vitro* MIC values when evaluated in both acute septicemia and neutropenic thigh infection models.** Fifty percent effective dose (ED_{50}) studies were conducted with LpxC-4 against *P. aeruginosa* UC12120, PA-1950, and PA-1955 and *K. pneumoniae* KP-1487 in an acute septicemia model. Efficacy, as assessed in this acute infection model, was generally consistent with MIC results, with ED_{50}s ranging from 7.4 mg/kg of body weight for PA-1950 (MIC = 0.25 μg/ml) to 55.9 mg/kg for PA-1955 (MIC = 2 μg/ml). We also established a strong correlation between the expression of *P. aeruginosa* LpxC-4 resistance determinants and *in vivo* efficacy by demonstrating that PA-1955 Δ*oprN* (MIC = 1 μg/ml) had an ED_{50} that was reduced to 19.8 mg/kg and that the PA-1955 sRNA mutant (MIC = 64 μg/ml) had an ED_{50} that was >200 mg/kg. To further define the exposure-effect relationship of these data, the ED_{50} data were normalized to an EC_{50} accounting for free drug concentrations in these studies. Pharmacokinetics of LpxC-4 following single subcutaneous doses of 18.75, 75, and 300 mg/kg revealed that exposure was generally linear across the dose range, with area under the concentration-time curve (AUC) and maximum concentration of drug in serum (C_{max}) increasing with a proportional increase in dose (Table 3). C_{max} values ranged from 5.02 to 75.4 μg/ml for doses from 18.75 to 300 mg/kg, respectively. Accounting for a free fraction of 0.31 (12), unbound LpxC-4 AUCs ranged from 1.58 to 23.7 μg·h/ml. *In vivo* pharmacokinetic/pharmacodynamic (PK/PD) driver and exposure magnitude determinations were characterized in a neutropenic thigh infection model with *K. pneumoniae* KP-1487 and *P. aeruginosa* UC12120. Dose fractionation of LpxC-4 suggested that the free AUC/MIC ratio (free AUC/MIC) was the variable most dynamically linked to efficacy against UC12120, with r^2 values of 0.79, 0.75, and 0.53 for free AUC/MIC, free C_{max}/MIC, and the percentage of the dosage interval in which the level of drug in serum exceeds the MIC (% time > MIC), respectively. Although data were more variable for activity against KP-1487, free AUC/MIC still showed the strongest correlation to activity, with r^2 values of 0.58, 0.51, and 0.21 for free AUC/MIC, free C_{max}/MIC, and % time > MIC, respectively. Endpoint studies of activity against PA-1950 and KP-1487 in the neutropenic thigh model suggested free AUC/MICs of 6.48 and 5.36, respectively, to reach the stasis (no net change in bacterial burden over 24 h) target. Free AUC/MICs of 7.25 and 13.5 were associated with a 1-log kill versus PA-1950 and KP-1487, respectively (Table 4). While EC_{50}s and targets for stasis and 1-log kill were broadly consistent across neutropenic thigh studies with *P. aeruginosa* and *K. pneumoniae*, the KP-1487 P22S FabZ mutant, which showed an 8-fold increase in the MIC versus that for wild-type KP-1487, demonstrated much lower AUC/MICs for PK/PD endpoints of stasis and 1-log kill, suggesting that these mutants are more susceptible *in vivo* than their *in vitro* MICs would suggest.

TABLE 3 Pharmacokinetics of LpxC-4 in CD-1 mice[a]

Parameter[b]	Value for dose (mg/kg) of:		
	18.75	75	300
C_{max} (mg/liter)	5.02 ± 0.61	15.50 ± 4.26	75.40 ± 5.65
T_{max} (h)	0.25 ± 0.00	0.33 ± 0.13	0.33 ± 0.13
AUC (mg · h/liter)	5.09 ± 1.04	17.60 ± 2.49	76.30 ± 0.96
Free AUC (mg · h/liter)	1.58 ± 0.32	5.46 ± 0.77	23.70 ± 0.30
Half-life (h)	0.60 ± 0.03	0.69 ± 0.03	0.68 ± 0.03
CL (liters/h/kg)	3.79 ± 0.78	4.32 ± 0.67	3.92 ± 0.04
V_{ss} (liters/kg)	2.20 ± 0.19	3.30 ± 0.55	2.53 ± 0.39

[a] Values are means ± SD.
[b] CL, clearance; V_{ss}, volume of distribution at steady state.

TABLE 4 In vivo efficacies (24-h AUC/MIC) of LpxC-4 in CD-1 mice against sentinel strains of *P. aeruginosa* and *K. pneumoniae*

Strain	MIC (μg/ml)	Immunocompetent septicemia EC_{50}[a]	Neutropenic lung EC_{50}	Neutropenic thigh stasis[a]	Neutropenic thigh 1-log kill[a]
P. aeruginosa					
UC12120	1	1.23 ± 2.34	NT[b]	NT	NT
PA-1950	0.25	6.31 ± 2.51	<8.40	6.48 ± 2.68	7.25 ± 20.32
PA-1955	2	5.00 ± 5.36	NT	NT	NT
PA-1955 Δ*oprN*	1	1.02 ± 0.68	NT	NT	NT
PA-1955 sRNA mutant	64	NC[c]	NT	NT	NT
K. pneumoniae					
KP-1487[d]	1	NT	NT	5.36 ± 0.49	13.50 ± 2.20
KP-1487[e]	1	NT	NT	14.50 ± 6.20	NC
KP-1487 FabZ P22S[d]	8	NT	NT	1.83 ± 2.69	3.45 ± 2.11

[a] Mean AUC/MIC ± SE.
[b] NT, not tested.
[c] NC, not calculable (ED_{50} > 200 mg/kg).
[d] Inoculum = 1×10^6 CFU.
[e] Inoculum = 1×10^7 CFU.

Pulmonary infection model of activity against *P. aeruginosa* PA-1950. Efficacy of LpxC-4 in an acute (48-h) mouse pneumonia model was achieved against PA-1950 with an ED_{50} of <25 mg/kg. This result was consistent with an estimated LpxC-4 ED_{50} of 16.8 mg/kg against PA-1950 in the neutropenic thigh model. Normalizing the dose to free drug exposure and considering an MIC of 0.25 μg/ml, the ED_{50}s in the thigh and lung endpoint studies correspond to free AUC/MICs of 7.2 and 10.7, respectively, suggesting similar exposure requirements for both models.

DISCUSSION

Here we have reported the *in vitro* and *in vivo* characterization of a recently disclosed inhibitor of the Gram-negative LpxC enzyme, which has demonstrated the potential of this drug class to provide a new option in the clinical setting. During the course of our experimentation, we were fascinated to find that our lead compounds also served as reagents to better understand the basic physiology of the organisms that they target. Our assessment of LpxC-4 resistance in multiple Gram-negative pathogens has demonstrated how differently many of the basic cellular processes are carried out in these organisms. For example, the fact that efflux is the preferred first-step resistance mechanism in *P. aeruginosa* but not *K. pneumoniae* is reflective of the functional distinction between the various RND efflux pumps produced by these bacterial species. Despite the fact that members of the *Enterobacteriaceae* produce AcrAB-TolC, an efflux pump whose substrate specificity includes several different classes of antibiotics (27) and therefore contributes to multidrug resistance, we have never established that LpxC-4 resistance can be achieved by overexpression of this system. This conclusion was based both on our inability to recover any spontaneously resistant mutants with increased production of AcrAB-TolC and the fact that clinical isolates known to have upregulated efflux expression (included in the MIC_{90} panels described in Table 1) did not demonstrate an increase in the LpxC-4 MIC. As a result, organisms such as *K. pneumoniae* require mutations in *fabZ* to resist the action of LpxC-4, much as *E. coli* does to resist other LpxC inhibitors described previously (26).

Since FabZ acts on *R*-3-hydroxymyristoyl acyl carrier protein, a substrate common to both lipid A and fatty acid biosynthesis, we and others (26) have hypothesized that these various *fabZ* point mutations result in a redistribution of the availability of this precursor, shunting more of it toward lipid A biosynthesis. More recently, however, it was demonstrated that CHIR-090-resistant *E. coli* mutants, each of which harbored a single point mutation within *fabZ*, showed a marked decrease in *lpxC* expression relative to that of their parent strain (28). These results support the contention that *E. coli* carefully regulates the coordinate expression of both lipid A and fatty acid biosynthetic pathways, since homeostasis between these two cellular components is vital to the survival of the organism. Our discovery that *fabZ*-mutated *K. pneumoniae* isolates display a skipped-well phenotype in MIC profiling studies reinforces this point, since reduced LpxC levels as a consequence of *fabZ* mutation result in fewer target molecules for LpxC-4 to inhibit. Intriguingly, our initial *in vivo* efficacy data with KP-1487 suggest that the apparent 8-fold MIC shift demonstrated by *fabZ* mutants *in vitro* does not translate to reduced susceptibility in an *in vivo* infection model. FOR and subsequent MIC profiling using similar LpxC compounds in our laboratories against *E. coli* revealed *fabZ* mutation as the primary resistance mechanism employed by this pathogen. Similarly to *K. pneumoniae*, these mutants also displayed the skipped-well pattern of growth. Whether these *E. coli* FabZ mutant strains retain *in vivo* susceptibility, in spite of an increase in MIC, is unknown at this time but warrants further investigation.

Another key difference between *P. aeruginosa* and members of the *Enterobacteriaceae* is the effect of LpxC overexpression and the regulatory mechanism employed by the former to control the levels of this enzyme. It has long been established that overproduction of LpxC has deleterious effects on bacterial cell survival, a consequence that is carefully avoided in the *Enterobacteriaceae* by the expression and activity of FtsH, an AAA protease that recognizes a specific C-terminal sequence in LpxC (29). The C terminus of *P. aeruginosa* LpxC does not include this recognition sequence, however, and this protein was recently shown not to be subjected to FtsH-mediated cleavage (30), a finding that has left the mechanism(s) of LpxC regulation a mystery in this organism. The recent identification of an sRNA upstream of *lpxC* in *P. aeruginosa* (21, 22), together with the repeated identification of spontaneous LpxC inhibitor-resistant strains harboring the exact same mutation within this RNA coding region, has provided some preliminary clues to better understand this novel mechanism of LpxC control. Since sRNA-mediated regulation can occur by direct binding via sequence complementarity, we attempted studies to demonstrate that C-to-A mutant sRNAs showed differential binding capabilities relative to wild-type sRNAs. Likewise, since sRNAs can regulate their targets through the recruitment of proteins, we also tested wild-type and mutant sRNAs for their ability to differentially bind to *P. aeruginosa* cellular extracts. In both cases we were unable to conclusively identify further mechanisms by which this sRNA controls *lpxC* expression, although optimization of experimental conditions could provide different results in the future. However, we were able to show that this upstream mutation leads to an increase in transcription of *lpxC*, rather than just its translation as has been proposed previously. The existence of this sRNA-mediated regulation in *P. aeruginosa* distinguishes it from members of the *Enterobacteriaceae*, and this difference is further supported by the lack of LpxC-overexpressed mutants recovered from FOR experiments with *K. pneumoniae*. The latter point may be explained by the significant sequence divergence upstream of *lpxC* between these pathogens. Whether LpxC overproduction in *P. aeruginosa* is better tolerated than it is in the *Enterobacteriaceae* remains to be understood and warrants further investigation.

In relevant *in vivo* models of infection, LpxC-4 was shown to be efficacious against sentinel strains of *P. aeruginosa* and *K. pneumoniae*. Activity in these models was commensurate with MIC values of the wild-type strains evaluated. PK/PD driver analysis suggested free AUC/MIC to be the parameter most closely linked to efficacy, and magnitude requirements for stasis and 1-log kill were determined. Magnitude requirements for a 1-log kill were nearly equivalent for PA-1950 and KP-1487, suggesting similar exposure targets to treat strains of *Pseudomonas* and *Klebsiella*. Certainly a greater number of strains will need to be studied to confirm exposure requirements, but based upon preliminary allometric scaling of preclinical PK (data not shown), a clinical dose of approximately 1,200 mg every 8 h (q8h) would be anticipated to sufficiently treat strains with MICs of 1 μg/ml or less. Additionally, if PA-1955 susceptibility (MIC = 2 μg/ml) is representative of first-step efflux mutants, it is likely that compounds like LpxC-4 could be used clinically against these *P. aeruginosa* strains as well. Unfortunately, our data do not suggest that LpxC-4 can effectively

treat second-step *P. aeruginosa* sRNA mutants with increased LpxC expression, although the frequency of these mutations is quite low and thus far they seem to arise only in strains with preexisting upregulated efflux expression. Therefore, we anticipate that the incidence at which these double mutants would spontaneously arise would be quite rare, although careful monitoring for the emergence of second-step-resistant mutants would be particularly critical for strains with efflux upregulation. Our data also support the conclusion that effective treatment against *K. pneumoniae* strains and likely other members of the *Enterobacteriaceae*, such as *E. coli*, that resist LpxC-4 through *fabZ* point mutation is achievable *in vivo*, despite the significant MIC shifts seen *in vitro*. This serves as yet another example in which the constraints of standardized *in vitro* susceptibility testing can hinder our ability to truly appreciate the potential for our candidate compounds by not accounting for the substantial differences in cell physiology in the harsh, nutrient-restricted *in vivo* environment versus that under nutrient-replete conditions used for classical MIC testing.

The need for new antibiotics, particularly those with novel mechanisms of action to minimize the prevalence of existing resistance, has prompted us to identify and evaluate a novel series of LpxC inhibitors for the treatment of serious Gram-negative infections. The results described in this report demonstrate that LpxC-4 is a potent, broad-spectrum inhibitor against which spontaneous resistance arises fairly infrequently. *In vivo* efficacy studies confirm our *in vitro* activity findings for multiple Gram-negative pathogens, and PK assessments suggest that the increases in the MIC associated with the major first-step resistance mechanism in *P. aeruginosa* may still be covered by realistic LpxC-4 dosing regimens. In addition, our identification and characterization of the skipped-well phenomenon displayed by *fabZ*-mutated *K. pneumoniae* first-step mutants also support the notion that major resistance mechanisms employed by *Enterobacteriaceae* may also be successfully treated by LpxC-4 *in vivo*. This unusual susceptibility phenotype, along with the preliminary work to describe the novel sRNA-mediated mechanism of *lpxC* regulation by *P. aeruginosa*, were discoveries that stemmed from the use of our LpxC inhibitors. The utilization and application of antibacterial agents as tools to further our understanding of the fundamental physiological processes used by target bacterial species is an important advancement that has the potential to provide valuable insight into novel antibiotic targets and pathways in the future.

MATERIALS AND METHODS

Bacterial strains and media used. Bacterial strains used in this study were from the Pfizer internal collection, consisting primarily of strains recovered from patients worldwide since 2000. *P. aeruginosa* PAO1 (provided by Mike Vasil, University of Colorado, Denver), UC12120, and PA-1950 are all antibiotic-susceptible strains, while strain PA-1955 is a MexEF-OprN-producing isolate recovered from a cystic fibrosis patient in 2000. *P. aeruginosa* PAO397 is a derivative of PAO1 that has deletion mutations in 5 major RND-type efflux pumps (31). *K. pneumoniae* strain KP-1487, an MDR clinical isolate that expresses KPC-2, SHV-12, and TEM-1, was obtained from New York-Presbyterian Hospital (Columbia University Medical Center). All strains were routinely grown and maintained on lysogeny broth (LB) and agar. All MIC, static time-kill (STK), and frequency-of-resistance (FOR) experiments were conducted in cation-adjusted Mueller-Hinton broth (caMHB), which was purchased from Difco. Where appropriate, medium was supplemented with 15 μg/ml (for *E. coli*) or 75 μg/ml (for *P. aeruginosa*) gentamicin.

LpxC inhibitor IC_{50}, MIC, and STK testing. Enzyme inhibition of each LpxC compound (shown in Fig. 1) was conducted using a functional LpxC enzyme assay, described previously (12). LpxC-4, which can be purchased commercially (catalog number PZ0194; Sigma-Aldrich), is also known as PF-5081090. MIC assays were conducted according to the guidelines established by the Clinical and Laboratory Standards Institute (CLSI) (32, 33). Where indicated, the efflux pump inhibitor phenylarginyl-β-naphthylamide (PAβN) (Sigma) was added at a final concentration of 50 μg/ml. STK assays were also conducted in accordance with CLSI guidelines. Briefly, a 0.5 McFarland suspension from an overnight LB agar plate was diluted to 5×10^5 in caMHB and incubated at 35°C with ambient atmosphere at 220 rpm for 90 min. STK assessments were carried out in 10 ml of preincubated culture with a range of concentrations of LpxC inhibitors. Samples (200 μl/sample) were collected at 0, 2, 4, 6, 8, 10, 24, and 48 h, serially diluted in phosphate-buffered saline, and spotted on blood agar plates before overnight incubation at 37°C for CFU/ml determinations.

FOR determination and resistant isolate characterization. Frequencies of resistance (FORs) were calculated using standard population analysis as described previously (6). Specifically, bacterial strains were grown in caMHB to mid-log phase (optical density at 600 nm [OD_{600}] = 0.5) prior to being concentrated 40× in fresh medium. One hundred microliters of this suspension (~1×10^9 CFU) was plated on agar plates containing increasing concentrations of LpxC inhibitors, ranging from 0.5 to 64 μg/ml (in 2-fold increments). Plates were incubated at 37°C for 40 h prior to colony counting. Resistance frequencies were calculated by dividing the number of colonies by the density of cells plated from the initial inoculum. Resistance stability of the recovered colonies was assessed by streaking on drug-free medium, freezing at −80°C, restreaking on drug-free medium, and using those grown colonies to conduct standard MIC testing. Isolates that demonstrated elevated MICs above those for the parent strain were further characterized to determine the mechanism of resistance.

FOR-generated isolates were initially characterized by conducting MICs in the presence and absence of PAβN. Total cell lysates were prepared by harvesting log-phase-grown LB cultures (OD_{600} = 0.5) and centrifuging an equivalent number of cells for each strain. Cell pellets were resuspended in 100 μl of phosphate-buffered saline (PBS) plus 100 μl 2× SDS-PAGE sample buffer (containing 5% β-mercaptoethanol), and samples were sonicated briefly prior to incubation at 100°C for 5 min. Lysate samples were separated by SDS-PAGE and subjected to Western blot analyses using OprM-, OprN-, and OprJ-specific monoclonal antibodies. Lysates were also probed with either a *P. aeruginosa* or *K. pneumoniae* anti-LpxC-specific antiserum. The full-length *lpxC* gene (including the upstream region) was PCR amplified and sequenced from these isolates using the primers PA LpxC.F (5′ ATCAGGAGTAGAGATGTG 3′) and PA LpxC.R (5′ AGAGGCCACCCTGAGGTG 3′) for *P. aeruginosa* and KP LpxC.F (5′ CATATGATCAAACAAAGGACTCTTAAA 3′) and LpxC.R (5′ GGATCCTTACGCCAGAACCATCGAC 3′) for *K. pneumoniae*. *K. pneumoniae* strains were also PCR amplified and sequenced with the *fabZ*-specific primers FabZ.F (5′ TTGACTACTGACACTCATACTCT GCAC 3′) and FabZ.R (5′ TCAGGCCTCCCGGCTACG 3′).

Mutagenesis of *oprN*. In order to generate OprN deletion mutants in *P. aeruginosa*, an internal portion of the *oprN* gene was PCR amplified from *P. aeruginosa* PAO1 genomic DNA using the primers OprN.F (5′ G CGCAGTCGATCCGGAGC 3′) and OprN.R (5′ GCGCTCCTGGCGCT TGCC 3′), and the resulting amplicon was cloned into pCR2.1-TOPO (Life Technologies). Digestion with HincII removed an internal 401-bp fragment of *oprN*, and the SmaI-digested Gm^R cassette from pPS856 (34) was ligated in its place. The region containing *oprN*::Gm^R was excised from pCR2.1-TOPO using PvuII and ligated into SmaI-digested pEX100T (35), and the resulting plasmid was transformed into *E. coli* Top10 (Life Technologies). This strain was used as the donor in a triparental mating with various recipient *P. aeruginosa* strains and *E. coli* HB101 harboring pRK2013 (36), which served as the helper plasmid. Gentamicin-

containing pseudomonas isolation agar (PIA) (Difco) was used to initially select for single-crossover mutants. Isolated colonies from this plate were collected and restruck for isolation on LB agar plates containing gentamicin and 5% sucrose, the latter of which was included to select for cells that had undergone a double-crossover recombination event. Finally, Gm^r and sucrose-resistant mutants were confirmed to be cured of pEX100T by plating on LB agar plates containing 500 μg/ml carbenicillin, and mutations were confirmed by DNA sequencing using target gene-specific primers. All restriction enzymes were purchased from New England Biolabs.

Analysis of *lpxC* upstream region and backcrossing into *P. aeruginosa*. The intergenic region separating *ftsZ* and *lpxC* was analyzed for the presence of a small RNA (sRNA) using the mfold server (http://mfold.rna.albany.edu). The contributions of mutations in this region to LpxC compound resistance were confirmed by backcrossing individual base changes into PAO397, a PAO1 isogenic mutant that cannot produce the MexAB-OprM, MexEF-OprN, MexCD-OprJ, MexXY, and MexJK efflux pumps (11). The primers LpxC.IG.For (5′ ATGGCGATGATGGGTACC 3′) and LpxC.IG.Rev (5′ GAACTCGTCCTCGTAACG 3′) were used to PCR amplify a 1,333-bp fragment from genomic DNA from both wild-type PA-1955 and a FOR-generated LpxC-4^R mutant of PA-1955, which harbors a C-to-A base change 11 bp upstream of the translational start site of *lpxC*. Each amplicon was cloned into pEX18ApGW (37), and the C-to-A-mutated allele was introduced into PAO397 by conjugation. After primary selection on LB agar plates containing 100 μg/ml carbenicillin, exconjugates were counterselected on LB agar containing 5% sucrose and 0.5 μg/ml LpxC-4. $Sucrose^R$ and LpxC-4^R colonies were confirmed to be cured of pEX18ApGW by replica plating on LB agar containing 100 μg/ml carbenicillin. Successful C-to-A replacement at 11 bp upstream of *lpxC* was confirmed in carbenicillin-susceptible clones by PCR and sequencing. Backcrossed PAO397 strains were characterized by MIC testing and Western blot analysis as described above.

LpxC and sRNA stability and expressional analyses. To measure changes in RNA stability as a result of the mutated *lpxC* gene upstream noncoding region, *P. aeruginosa* strain PA-1955 and its isogenic C-to-A mutant, along with PAO397 and its backcrossed C-to-A mutant (described above), were grown to mid-logarithmic phase (OD_{600} = 0.45) in LB with shaking. Transcription was halted through the addition of 200 μg/ml rifampin, and total RNA was extracted at both 0 and 5 min posttreatment. qRT-PCR was conducted according to the $2^{-\Delta\Delta CT}$ method (38) using the primers lpxC.F (5′ AAGAAGTTCATCCGCATCA AGCGC 3′) and lpxC.R (5′ CCTCCTTGACGAAGGAAGTACTGG 3′) and rpsL.F (5′ GCAAGCGCATGGTCGACAAGA 3′) and rpsL.R (5′ CG CTGTGCTCTTGCAGGTTGTGA 3′), the latter of which served as an internal control. Triplicate samples were analyzed, and changes in relative expression levels found in C-to-A mutants were expressed as fold changes over their respective parent strains.

Pharmacokinetic studies and analysis. LpxC-4 pharmacokinetic properties were determined in neutropenic female CF-1 mice with active thigh infections. Plasma exposure was determined following subcutaneous dosing at dose levels of 18.75, 75, and 300 mg/kg. Animals (n = 3/time point/dose level) were administered doses in 40% cyclodextrin at a dose volume of 0.2 ml. Terminal blood samples were taken via cardiac puncture at 0.25, 0.5, 1, 2, 4, 6, and 8 h postdose, collected into disodium EDTA Microtainers (BD Biosciences, Franklin Lakes, NJ), and processed for plasma. Concentrations of LpxC were determined by liquid chromatography-tandem mass spectrometry (LC-MS/MS). Briefly, plasma samples (50 μl) were subjected to protein precipitation with acetonitrile (200 μl) containing an internal standard (diclofenac; Sigma-Aldrich St. Louis, MO), and 5 μl of the resulting supernatant was injected onto a Luna C_{18} column (2.7 μm, 30 × 3 mm; Phenomenex, Torrance, CA). The column was equilibrated with solution A (95:5 water-acetonitrile, 0.1% acetic acid) at a flow rate of 1.0 ml/min. The gradient was started at 5% solution B (95:5 acetonitrile-water, 0.1% acetic acid) and was increased to 95% solution B from 0.5 to 1.5 min. Conditions were held at 95% solution B until 2.0 min and then returned to starting conditions by 2.3 min and held for an additional 0.5 min for a total run time of 2.8 min. The effluent was analyzed with an API-4000 mass spectrometer detector (AB Sciex, Foster City, CA), fitted with a turbo ion spray interface and operated in the negative-ion mode. LpxC-4 and diclofenac were detected by multiple reactions monitoring at transitions 410.9/330.8 and 293.9/249.9, respectively. The dynamic range of the assay was 2.5 ng/ml to 10 μg/ml for LpxC-4.

LpxC-4 concentrations (mean data for three mice per time point were used to generate a single concentration-time curve) were fitted to a 1-compartment model using the software program WinNonLin, version 5.2 (Pharsight, St. Louis, MO). The maximum concentration (C_{max}) was the highest observed concentration; T_{max} was the earliest time at which C_{max} occurred; and the elimination half-life was estimated as ln2/*k*el, where *k*el is the elimination rate constant derived from the slope of the log concentration-versus-time profile. The area under the concentration-time curve from 0 h to the last time point (AUC_0–t_{last}) was calculated by linear trapezoidal approximation.

General *in vivo* procedures. All animal experiments were conducted in accordance with regulations and established guidelines and were reviewed and approved by the Pfizer Institutional Animal Care and Use Committee. Comparative efficacy and dose response were determined in an immunocompetent model of septicemia. Exposure-effect and PK/PD driver assessments were determined using PA-1950 and KP-1487 as representative clinical strains in a neutropenic thigh and lung pneumonia model. Animals were housed in groups of 5 to 10 mice per cage and given access to food and water *ad libitum* for all studies. For immunosuppression studies, animals were rendered transiently neutropenic by administration of two oral doses of cyclophosphamide monohydrate (Sigma-Aldrich, St. Louis, MO). The first dose (150 mg/kg in 0.2 ml sterile water) was administered 4 days prior to infection, and the second dose (100 mg/kg in 0.2 ml sterile water) was administered 1 day prior to infection.

Acute septicemia model. Groups of five CF-1 female mice (Charles River Laboratories) were infected intraperitoneally with *P. aeruginosa* and *K. pneumoniae* strains diluted in 3% brewer's yeast (Sigma-Aldrich, St. Louis, MO). Inocula were prepared from frozen stock with 100 μl spread on sheep blood agar plates and incubated overnight at 37°C. The resulting colonies were harvested, washed with brain heart infusion broth (BHIB), and diluted to a target inoculum of ~1 × 10^4 CFU/mouse delivered in 0.5 ml. Mice were treated with LpxC-4 at 0.5 h and 4 h postinfection. The compound was administered subcutaneously (s.c.) in a dose volume of 0.2 ml. Doses ranged from 0 to 100 mg/kg, and the compound was reconstituted in 40% cyclodextrin in sterile water prior to administration. Animals were euthanized at the onset of therapy and 24 h post-bacterial challenge, spleens were surgically excised, and bacterial colonies were enumerated by standard plate counting methods (CFU/spleen) on MacConkey's agar for cultivation. Efficacy was established as the difference in bacterial burden over 24 h and applied to fractional dose-response model with the following characteristics: 24-h maximum effect (E_{max}) = lower limit of detection − 0-h log CFU; 24-h minimum effect (E_{min}) = 0-h CFU − 24-h upper limit of detection; 0-h mean = average log CFU at onset of therapy. The fractional response (%) = (24-h delta log CFU − E_{min})/(E_{max} − E_{min}). ED_{50} values were determined from nonlinear regression analysis of the fractional dose-response using the software program GraphPad Prism, version 3.02 (GraphPad Software, La Jolla, CA).

Neutropenic thigh infection model. CF-1 female mice were rendered transiently neutropenic as described above and challenged with 0.1 ml of a 1:1 ratio of Cytodex beads (lot 124H0068; Sigma): 10^{-4} dilution of plate-scraped PA-1950 or KP-1487. The inocula were delivered intramuscularly into the left femoral bicep of CF-1 mice. Subcutaneous therapy was initiated 1 h following bacterial challenge using q24h, q12h, q6h, and q3h dosing intervals that covered a 64-fold dose range from 3.69 to 300 mg/kg/course of therapy. Efficacy was determined by assessing the bacterial burden at 0 and 24 h post-initiation of therapy (1 and 25 h post-bacterial challenge). Infected thighs were aseptically excised and processed for bac-

terial burden enumeration. The change in CFU over 24 h was determined for each dose level, and the data were analyzed by nonlinear regressional analysis.

Pulmonary infection model. Groups consisting of 8 isoflurane-anesthetized C3H/HeN female mice (Charles River Laboratories) were infected with *P. aeruginosa* PA-1950 by placing 40 μl of bacterial suspension in BHIB onto the external nares. Each mouse was held in a vertical position until the droplet was completely inhaled. The targeted inoculum was 1×10^6 CFU/animal. Therapy with LpxC-4 was initiated on day 1 of the study at 0.5 h post-bacterial challenge, and animals received an additional dose at 4 h post-challenge. This twice-daily dosing was repeated on day 2 of the study, animals were euthanized at 48 h post-challenge, and the lungs were aseptically removed and processed for bacterial burden enumeration. Efficacy was assessed as the difference in bacterial burden from the initiation of therapy to 48 h post-challenge.

REFERENCES

1. **Sutcliffe JA, O'Brien W, Fyfe C, Grossman TH.** 2013. Antibacterial activity of eravacycline (TP-434), a novel fluorocycline, against hospital and community pathogens. Antimicrob. Agents Chemother. **57:** 5548–5558. http://dx.doi.org/10.1128/AAC.01288-13.
2. **Walkty A, Adam H, Baxter M, Denisuik A, Lagace-Wiens P, Karlowsky JA, Hoban DJ, Zhanel GG.** 2014. *In vitro* activity of plazomicin against 5,015 gram-negative and gram-positive clinical isolates obtained from patients in Canadian hospitals as part of the CANWARD study, 2011-2012. Antimicrob. Agents Chemother. **58:**2554–2563. http://dx.doi.org/10.1128/AAC.02744-13.
3. **Sader HS, Rhomberg PR, Farrell DJ, Jones RN.** 2011. Antimicrobial activity of CXA-101, a novel cephalosporin tested in combination with tazobactam against Enterobacteriaceae, *Pseudomonas aeruginosa*, and *Bacteroides fragilis* strains having various resistance phenotypes. Antimicrob. Agents Chemother. **55:**2390–2394. http://dx.doi.org/10.1128/AAC.01737-10.
4. **Nikaido H.** 2003. Molecular basis of bacterial outer membrane permeability revisited. Microbiol. Mol. Biol. Rev. **67:**593–656. http://dx.doi.org/10.1128/MMBR.67.4.593-656.2003.
5. **Delcour AH.** 2009. Outer membrane permeability and antibiotic resistance. Biochim. Biophys. Acta **1794:**808–816. http://dx.doi.org/10.1016/j.bbapap.2008.11.005.
6. **McPherson CJ, Aschenbrenner LM, Lacey BM, Fahnoe KC, Lemmon MM, Finegan SM, Tadakamalla B, O'Donnell JP, Mueller JP, Tomaras AP.** 2012. Clinically relevant Gram-negative resistance mechanisms have no effect on the efficacy of MC-1, a novel siderophore-conjugated monocarbam. Antimicrob. Agents Chemother. **56:**6334–6342. http://dx.doi.org/10.1128/AAC.01345-12.
7. **Page MG, Dantier C, Desarbre E.** 2010. *In vitro* properties of BAL30072, a novel siderophore sulfactam with activity against multiresistant gram-negative bacilli. Antimicrob. Agents Chemother. **54:**2291–2302. http://dx.doi.org/10.1128/AAC.01525-09.
8. **Onishi HR, Pelak BA, Gerckens LS, Silver LL, Kahan FM, Chen MH, Patchett AA, Galloway SM, Hyland SA, Anderson MS, Raetz CR.** 1996. Antibacterial agents that inhibit lipid A biosynthesis. Science **274:** 980–982. http://dx.doi.org/10.1126/science.274.5289.980.
9. **Mdluli KE, Witte PR, Kline T, Barb AW, Erwin AL, Mansfield BE, McClerren AL, Pirrung MC, Tumey LN, Warrener P, Raetz CR, Stover CK.** 2006. Molecular validation of LpxC as an antibacterial drug target in *Pseudomonas aeruginosa*. Antimicrob. Agents Chemother. **50:**2178–2184. http://dx.doi.org/10.1128/AAC.00140-06.
10. **Caughlan RE, Jones AK, Delucia AM, Woods AL, Xie L, Ma B, Barnes SW, Walker JR, Sprague ER, Yang X, Dean CR.** 2012. Mechanisms decreasing *in vitro* susceptibility to the LpxC inhibitor CHIR-090 in the gram-negative pathogen *Pseudomonas aeruginosa*. Antimicrob. Agents Chemother. **56:**17–27. http://dx.doi.org/10.1128/AAC.05417-11.
11. **Brown MF, Reilly U, Abramite JA, Arcari JT, Oliver R, Barham RA, Che Y, Chen JM, Collantes EM, Chung SW, Desbonnet C, Doty J, Doroski M, Engtrakul JJ, Harris TM, Huband M, Knafels JD, Leach KL, Liu S, Marfat A, Marra A, McElroy E, Melnick M, Menard CA, Montgomery JI, Mullins L, Noe MC, O'Donnell J, Penzien J, Plummer MS, Price LM, Shanmugasundaram V, Thoma C, Uccello DP, Warmus JS, Wishka DG.** 2012. Potent inhibitors of LpxC for the treatment of Gram-negative infections. J. Med. Chem. **55:**914–923. http://dx.doi.org/10.1021/jm2014748.
12. **Montgomery JI, Brown MF, Reilly U, Price LM, Abramite JA, Arcari J, Barham R, Che Y, Chen JM, Chung SW, Collantes EM, Desbonnet C, Doroski M, Doty J, Engtrakul JJ, Harris TM, Huband M, Knafels JD, Leach KL, Liu S, Marfat A, McAllister L, McElroy E, Menard CA, Mitton-Fry M, Mullins L, Noe MC, O'Donnell J, Oliver R, Penzien J, Plummer M, Shanmugasundaram V, Thoma C, Tomaras AP, Uccello DP, Vaz A, Wishka DG.** 2012. Pyridone methylsulfone hydroxamate LpxC inhibitors for the treatment of serious gram-negative infections. J. Med. Chem. **55:**1662–1670. http://dx.doi.org/10.1021/jm2014875.
13. **Barb AW, McClerren AL, Snehelatha K, Reynolds CM, Zhou P, Raetz CR.** 2007. Inhibition of lipid A biosynthesis as the primary mechanism of CHIR-090 antibiotic activity in Escherichia coli. Biochemistry **46:** 3793–3802. http://dx.doi.org/10.1021/bi6025165.
14. **Barb AW, Jiang L, Raetz CR, Zhou P.** 2007. Structure of the deacetylase LpxC bound to the antibiotic CHIR-090: time-dependent inhibition and specificity in ligand binding. Proc. Natl. Acad. Sci. U. S. A. **104:** 18433–18438. http://dx.doi.org/10.1073/pnas.0709412104.
15. **Lin L, Tan B, Pantapalangkoor P, Ho T, Baquir B, Tomaras A, Montgomery JI, Reilly U, Barbacci EG, Hujer K, Bonomo RA, Fernandez L, Hancock RE, Adams MD, French SW, Buslon VS, Spellberg B.** 2012. Inhibition of LpxC protects mice from resistant *Acinetobacter baumannii* by modulating inflammation and enhancing phagocytosis. mBio **3**(5): e00312-12. http://dx.doi.org/10.1128/mBio.00312-12.
16. **Moffatt JH, Harper M, Harrison P, Hale JD, Vinogradov E, Seemann T, Henry R, Crane B, St Michael F, Cox AD, Adler B, Nation RL, Li J, Boyce JD.** 2010. Colistin resistance in *Acinetobacter baumannii* is mediated by complete loss of lipopolysaccharide production. Antimicrob. Agents Chemother. **54:**4971–4977. http://dx.doi.org/10.1128/AAC.00834-10.
17. **Maseda H, Saito K, Nakajima A, Nakae T.** 2000. Variation of the mexT gene, a regulator of the MexEF-oprN efflux pump expression in wild-type strains of *Pseudomonas aeruginosa*. FEMS Microbiol. Lett. **192:**107–112. http://dx.doi.org/10.1111/j.1574-6968.2000.tb09367.x.
18. **Llanes C, Köhler T, Patry I, Dehecq B, van Delden C, Plésiat P.** 2011. Role of the MexEF-OprN efflux system in low-level resistance of *Pseudomonas aeruginosa* to ciprofloxacin. Antimicrob. Agents Chemother. **55:** 5676–5684. http://dx.doi.org/10.1128/AAC.00101-11.
19. **Evans K, Adewoye L, Poole K.** 2001. MexR repressor of the *mexAB-oprM* multidrug efflux operon of *Pseudomonas aeruginosa*: identification of MexR binding sites in the *mexA-mexR* intergenic region. J. Bacteriol. **183:** 807–812. http://dx.doi.org/10.1128/JB.183.3.807-812.2001.
20. **Zuker M.** 2003. Mfold web server for nucleic acid folding and hybridization prediction. Nucleic Acids Res. **31:**3406–3415. http://dx.doi.org/10.1093/nar/gkg595.
21. **Sonnleitner E, Sorger-Domenigg T, Madej MJ, Findeiss S, Hackermüller J, Hüttenhofer A, Stadler PF, Bläsi U, Moll I.** 2008. Detection of small RNAs in *Pseudomonas aeruginosa* by RNomics and structure-based bioinformatic tools. Microbiology **154:**3175–3187. http://dx.doi.org/10.1099/mic.0.2008/019703-0.
22. **Sonnleitner E, Haas D.** 2011. Small RNAs as regulators of primary and secondary metabolism in Pseudomonas species. Appl. Microbiol. Biotechnol. **91:**63–79. http://dx.doi.org/10.1007/s00253-011-3332-1.
23. **Winsor GL, Lam DK, Fleming L, Lo R, Whiteside MD, Yu NY, Hancock RE, Brinkman FS.** 2011. Pseudomonas Genome Database: improved comparative analysis and population genomics capability for Pseudomonas genomes. Nucleic Acids Res. **39:**D596–D600. http://dx.doi.org/10.1093/nar/gkq869.
24. **Hawley JS, Murray CK, Griffith ME, McElmeel ML, Fulcher LC, Hospenthal DR, Jorgensen JH.** 2007. Susceptibility of Acinetobacter strains isolated from deployed U.S. military personnel. Antimicrob. Agents Chemother. **51:**376–378. http://dx.doi.org/10.1128/AAC.00858-06.
25. **Schurek KN, Sampaio JL, Kiffer CR, Sinto S, Mendes CM, Hancock RE.** 2009. Involvement of *pmrAB* and *phoPQ* in polymyxin B adaptation and inducible resistance in non-cystic fibrosis clinical isolates of *Pseudomonas aeruginosa*. Antimicrob. Agents Chemother. **53:**4345–4351. http://dx.doi.org/10.1128/AAC.01267-08.
26. **Clements JM, Coignard F, Johnson I, Chandler S, Palan S, Waller A, Wijkmans J, Hunter MG.** 2002. Antibacterial activities and characterization of novel inhibitors of LpxC. Antimicrob. Agents Chemother. **46:** 1793–1799. http://dx.doi.org/10.1128/AAC.46.6.1793-1799.2002.
27. **Nikaido H.** 1998. Antibiotic resistance caused by gram-negative multi-

drug efflux pumps. Clin. Infect. Dis. **27**(Suppl 1):S32–S41. http://dx.doi.org/10.1086/514920.

28. **Zeng D, Zhao J, Chung HS, Guan Z, Raetz CR, Zhou P.** 2013. Mutants resistant to LpxC inhibitors by rebalancing cellular homeostasis. J. Biol. Chem. **288:**5475–5486. http://dx.doi.org/10.1074/jbc.M112.447607.
29. **Führer F, Langklotz S, Narberhaus F.** 2006. The C-terminal end of LpxC is required for degradation by the FtsH protease. Mol. Microbiol. **59:** 1025–1036. http://dx.doi.org/10.1111/j.1365-2958.2005.04994.x.
30. **Langklotz S, Schäkermann M, Narberhaus F.** 2011. Control of lipopolysaccharide biosynthesis by FtsH-mediated proteolysis of LpxC is conserved in enterobacteria but not in all gram-negative bacteria. J. Bacteriol. **193:**1090–1097. http://dx.doi.org/10.1128/JB.01043-10.
31. **Chuanchuen R, Murata T, Gotoh N, Schweizer HP.** 2005. Substrate-dependent utilization of OprM or OpmH by the *Pseudomonas aeruginosa* MexJK efflux pump. Antimicrob. Agents Chemother. **49:**2133–2136. http://dx.doi.org/10.1128/AAC.49.5.2133-2136.2005.
32. **CLSI.** 2009. Performance standards for antimicrobial susceptibility testing: 19th informational supplement, document M100-S17. CLSI, Wayne, PA.
33. **CLSI.** 2009. Methods for dilution antimicrobial susceptibility tests for bacteria that grow aerobically: approved standard, document M07. CLSI, Wayne, PA.
34. **Hoang TT, Karkhoff-Schweizer RR, Kutchma AJ, Schweizer HP.** 1998. A broad-host-range Flp-FRT recombination system for site-specific excision of chromosomally-located DNA sequences: application for isolation of unmarked *Pseudomonas aeruginosa* mutants. Gene **212:**77–86. http://dx.doi.org/10.1016/S0378-1119(98)00130-9.
35. **Schweizer HP, Hoang TT.** 1995. An improved system for gene replacement and xylE fusion analysis in *Pseudomonas aeruginosa*. Gene **158:** 15–22. http://dx.doi.org/10.1016/0378-1119(95)00055-B.
36. **Figurski DH, Helinski DR.** 1979. Replication of an origin-containing derivative of plasmid RK2 dependent on a plasmid function provided in trans. Proc. Natl. Acad. Sci. U. S. A. **76:**1648–1652. http://dx.doi.org/10.1073/pnas.76.4.1648.
37. **Choi KH, Schweizer HP.** 2005. An improved method for rapid generation of unmarked *Pseudomonas aeruginosa* deletion mutants. BMC Microbiol. **5:**30. http://dx.doi.org/10.1186/1471-2180-5-30.
38. **Livak KJ, Schmittgen TD.** 2001. Analysis of relative gene expression data using real-time quantitative PCR and the 2(-delta delta C(T)) method. Methods **25:**402–408. http://dx.doi.org/10.1006/meth.2001.1262.